International Journal for Multidisciplinary Research (IJFMR)
E-ISSN: 2582-2160 ● Website: www.ijfmr.com ● Email: editor@ijfmr.com

Formulation, Optimization, and In Vitro Evaluation of a Cassia tora Seed Extract (Chrysophanic Acid-9-Anthrone)-Loaded Nanoemulsion Gel for Topical Antifungal Delivery

Ms. Nikita Jayadeo Chaudhari[1], Dr. Suhas N Sakarkar[2], Prof. Pooja Ghutke[3]

[1]Student, Quality Assurance

Abstract

Background: Superficial cutaneous mycoses remain a widespread dermatological burden, and conventional topical antifungal creams and ointments are often limited by poor skin residence time, low aqueous solubility of active agents, and rising resistance among dermatophyte and mould species. Chrysophanic acid-9-anthrone, an anthraquinone principle isolated from the seeds of Cassia tora Linn., has documented antifungal activity but poor formulability restricts its topical use. Objective: To formulate, optimize, and evaluate a Cassia tora seed extract (chrysophanic acid-9-anthrone)-loaded oil-in-water nanoemulsion gel intended for topical antifungal delivery. Methods: Chrysophanic acid-9-anthrone was extracted from Cassia tora seeds by sequential Soxhlet defatting (petroleum ether) and extraction (benzene) and characterized for organoleptic, solubility, partition coefficient, loss on drying, melting point, UV/FTIR and TLC properties. Five oleic acid-in-water nanoemulsions (NE-A0–NE-A4) were prepared by high-speed homogenization/ultrasonication and screened for viscosity, droplet size, polydispersity index, and thermodynamic stability. The optimized nanoemulsion (NE-A1) was incorporated into Carbopol 934 hydrogel bases (1–4% w/w) to yield four nanoemulsion gels (NEG-1–NEG-4), which were characterized for pH, viscosity, spreadability, extrudability, swelling index and drug content, and evaluated for in vitro drug release across an egg-membrane diffusion model and antifungal activity against Aspergillus niger MTCC 282 by agar-well diffusion. The optimized gel (NEG-2) was subjected to a 3-month accelerated stability study. Results: NE-A1 showed the smallest mean droplet size (850.4 nm) and lowest viscosity (4240 cps) among thermodynamically stable batches. NEG-2 (2% w/w Carbopol 934) showed the most favourable overall profile (pH 6.39, spreadability 4.0 cm, drug content 93.55%) and released 42.6% of the loaded drug over 120 minutes, compared with 36.8–39.6% for the other gels. NEG-2 produced a concentration-dependent zone of inhibition against A. niger, rising from 8.7 mm at 25 µg/mL to 22.0 mm at 100 µg/mL, approaching the 26.0 mm zone of the amphotericin B reference standard. The optimized gel retained acceptable pH, viscosity and >90% drug content after 3 months at 37 °C/65% RH and 45 °C/75% RH. Conclusion: A Cassia tora-derived nanoemulsion gel is a technically

feasible, physicochemically stable, and antifungally active topical delivery system, supporting its further evaluation as a plant-derived alternative to conventional synthetic topical antifungals.

Keywords: Cassia tora; chrysophanic acid-9-anthrone; nanoemulsion gel; topical antifungal delivery; Aspergillus niger; herbal nanocarrier

1. Introduction

Superficial fungal infections of the skin, hair and nails affect an estimated one-quarter of the world's population at any given time, making dermatophytosis and related mycoses among the most common reasons for dermatological consultation worldwide [1]. These infections are rarely life-threatening but are persistent, disfiguring, and prone to relapse, and their burden is disproportionately high in warm, humid climates and in immunocompromised individuals [2].

The mainstay of management for localized superficial mycoses remains topical therapy with azole, allylamine or polyene antifungals delivered as creams, ointments or lotions. However, conventional semisolid vehicles frequently suffer from poor and inconsistent skin residence time, occlusive greasiness that discourages adherence, limited penetration of the stratum corneum by poorly water-soluble actives, and an expanding pattern of antifungal resistance and treatment failure, prompting continued interest in both improved vehicles and new active agents [3,4].

Plant-derived antifungal agents have re-emerged as an attractive complement or alternative to synthetic drugs because of their generally favourable safety profile, low cost, and the comparatively slower development of resistance against multi-component phytochemical mixtures [5]. Cassia tora Linn. (Fabaceae), a widely distributed weed used across South and Southeast Asia in traditional medicine, is one such candidate: seed and leaf extracts of C. tora have repeatedly demonstrated in vitro antifungal and antidermatophytic activity [6–8], which has been attributed largely to its anthraquinone constituents [9]. Among these, chrysophanic acid-9-anthrone, first isolated from C. tora seed as a fungicidal principle [10], together with related anthraquinone glycosides such as chrysophanol-1-β-gentiobioside and rubrofusarin glucosides [11,12], is regarded as a major contributor to the plant's antifungal activity, and the seed itself has a long history of use in traditional and folk pharmacopoeias [13,14].

Despite this pharmacological promise, chrysophanic acid-9-anthrone shares a limitation common to many lipophilic phytoconstituents: poor aqueous solubility and correspondingly poor partitioning into and across the skin when delivered from conventional semisolid or hydro-alcoholic vehicles, which constrains its practical antifungal efficacy in a simple cream or ointment base [15,16]. Nanoemulsion-based delivery systems — thermodynamically metastable, kinetically stable oil-in-water dispersions with droplet sizes generally below 1 µm — address this limitation by combining a high interfacial surface area, enhanced solubilization capacity for lipophilic actives, and improved capacity to modulate stratum corneum lipid packing, which together favour more consistent and enhanced cutaneous drug delivery relative to conventional vehicles [17–19]. Converting a nanoemulsion into a gel by incorporation into a hydrophilic polymer matrix such as Carbopol further improves its rheological behaviour, spreadability, and skin residence time while retaining the internal-phase advantages of the nanoemulsion, an approach already reported for several synthetic antifungal and anti-inflammatory actives [20–23].

Although nanoemulsion and nanoemulsion-gel systems have been explored for a range of synthetic drugs [24,25], and the antifungal activity of C. tora extracts has been independently documented, no report to date has combined the two — that is, formulated chrysophanic acid-9-anthrone isolated from C. tora seed

into an optimized nanoemulsion gel and evaluated its performance as a topical antifungal system. The present study was therefore designed to (i) extract and characterize chrysophanic acid-9-anthrone from C. tora seed; (ii) develop and optimize an oil-in-water nanoemulsion of the extract and incorporate it into a Carbopol 934 gel base; (iii) characterize the resulting nanoemulsion gel for its physicochemical and rheological properties; and (iv) evaluate its in vitro drug release and antifungal activity against Aspergillus niger, together with its short-term stability, to establish proof of concept for this plant-derived nanocarrier as a topical antifungal alternative.

2. Materials and Methods

2.1 Plant material and chemicals

Seeds of Cassia tora Linn. were collected in the month of December, authenticated, washed, shade-dried and powdered. Tween 80, Span 80, oleic acid, polyethylene glycol (PEG-400), Carbopol 934, triethanolamine and propylene glycol were procured as standard laboratory-grade reagents; petroleum ether (60–80 °C) and benzene (analytical grade) were used as extraction solvents. Aspergillus niger MTCC 282 was used as the challenge organism for antifungal evaluation.

2.2 Extraction and isolation of chrysophanic acid-9-anthrone

Shade-dried, powdered seeds (sieve #10) were first defatted by continuous hot extraction with petroleum ether (60–80 °C) in a Soxhlet apparatus. The defatted marc was air-dried to remove residual solvent, repacked, and extracted exhaustively with benzene in the same apparatus. The benzene extract was filtered, concentrated on a water bath, dried, and stored in an air-tight container at a cool place; percentage yield was calculated gravimetrically at each stage.

2.3 Preformulation characterization

The dried extract was characterized for organoleptic properties (colour, odour, texture), solubility in water and common organic solvents, oil–water partition coefficient, loss on drying, melting point (capillary method), and thin-layer chromatographic Rf value. Structural/functional-group identity was confirmed by FTIR spectroscopy (KBr pellet, 4000–400 cm^{-1}), and a UV spectrophotometric calibration curve was constructed in the 200–400 nm range to support subsequent drug-content and release-study quantification.

2.4 Selection of oil, surfactant and co-surfactant

Screening of the oil phase was performed by assessing extract solubility in mineral oil, fixed vegetable oil, olive oil, and oleic acid, with oleic acid selected on the basis of maximal solubilization without precipitation. Tween 80 (surfactant) and PEG-400 (co-surfactant) were selected on the same solubility/compatibility basis for the aqueous surfactant mixture (Smix).

2.5 Preparation of the nanoemulsion

Oil-in-water nanoemulsions were prepared by the aqueous phase titration/high-shear homogenization method followed by probe ultrasonication. The oil phase (oleic acid, with or without dissolved extract) was added dropwise to the aqueous Smix (Tween 80 : PEG-400) under continuous stirring, followed by ultrasonication at defined amplitude and time to reduce droplet size. Five batches (NE-A0–NE-A4) were prepared by varying the oil-phase concentration, Smix ratio, sonication amplitude and sonication time, as summarized in Table 1; NE-A0 was an excipient-only (drug-free) control.

Batch	Extract (%)	Oleic acid (%)	Smix (%)	Amplitude (%)	Sonication time (min)
NE-A0	—	5	15	100	5
NE-A1	1.0	5	15	100	5
NE-A2	1.0	5	10	100	8
NE-A3	0.5	7.5	5	80	5
NE-A4	1.0	10	10	50	5

Table 1. Composition and process variables of nanoemulsion batches NE-A0–NE-A4.

2.6 Characterization of the nanoemulsion

Each batch was evaluated for viscosity (Brookfield-type viscometer), mean droplet size and polydispersity index (dynamic light scattering, Z-average), and thermodynamic stability by centrifugation (5000 rpm, 30 min), heating–cooling cycles (4 °C/45 °C, ≥6 cycles) and freeze–thaw cycles (−21 °C/25 °C, 3 cycles); phase separation, creaming or drug precipitation at any stage was scored as failure.

2.7 Preparation of Carbopol 934 gel and nanoemulsion gel

Carbopol 934 was dispersed in water at 1–4% w/w (batches GF-1 to GF-4) and neutralized with triethanolamine to obtain blank gel bases; viscosity was measured to select the working Carbopol concentration range. The optimized nanoemulsion (NE-A1) was then incorporated into Carbopol 934 gel bases at four different polymer concentrations to yield four nanoemulsion gel formulations (NEG-1–NEG-4), each standardized to contain 2.5% w/w nanoemulsion, with propylene glycol as humectant.

2.8 Characterization of the nanoemulsion gel

NEG-1–NEG-4 were evaluated for physical appearance and homogeneity, pH (digital pH meter, 1% w/v aqueous dispersion), viscosity (Brookfield viscometer, spindle/speed held constant across batches), spreadability (parallel-plate slip-and-drag method), extrudability (weight required to extrude a fixed ribbon length from a collapsible tube, expressed as g/cm²), percentage swelling index, and drug content (UV spectrophotometric assay against the calibration curve, after appropriate dilution).

2.9 In vitro drug release study

Drug release from each nanoemulsion gel was assessed using a Franz-type diffusion set-up with an egg-membrane barrier mounted between donor and receptor compartments, receptor medium maintained under sink conditions and constant stirring at 37 ± 0.5 °C. Aliquots were withdrawn at fixed intervals (5, 10, 15, 20, 25, 30, 60, 90 and 120 min), replaced with equal volumes of fresh medium, and analysed spectrophotometrically; cumulative percentage drug release was plotted against time.

2.10 In vitro antifungal activity

Antifungal activity of the optimized gel (NEG-2) was assessed against Aspergillus niger MTCC 282 by the agar-well diffusion method on Sabouraud dextrose agar. Wells were loaded with gel equivalent to 25, 50, 75 and 100 µg/mL of extract; amphotericin B (10 µg/mL) served as the reference standard and untreated gel base as the negative control. Plates were incubated at 25 ± 2 °C for 72–96 h and the diameter of the zone of inhibition was measured in triplicate.

2.11 Stability studies

The optimized nanoemulsion gel (NEG-2) was packed in collapsible tubes and stored under three conditions — 37 ± 2 °C/65% RH, 45 ± 2 °C/75% RH, and 60 ± 2 °C — in accordance with ICH accelerated

stability guidance. Samples were withdrawn at 1, 2 and 3 months and re-evaluated for pH, viscosity, and drug content.

2.12 Statistical analysis

All characterization, release and antifungal assays were performed in triplicate (n = 3) unless otherwise stated; results are expressed as mean ± standard deviation (SD).

3. Results and Discussion

3.1 Extraction and preformulation characterization

Sequential Soxhlet processing of 31.11 g of powdered C. tora seed reduced the marc to 29.44 g after petroleum-ether defatting and to 27.62 g of exhausted marc following subsequent benzene extraction; the dried benzene extract recovered therefore weighed 1.82 g, corresponding to an extractive yield of approximately 5.85% w/w of the starting powder mass. This yield is consistent with the typically low proportion of anthraquinone-rich extractable material recovered from seed matrices once non-polar fixed-oil contaminants have been removed by preliminary defatting. The isolated extract was a yellowish-brown, crystalline solid with a characteristic odour, sparingly soluble in water and freely soluble in benzene, chloroform and ethanol, in line with its expected anthraquinone character. Key preformulation parameters are summarized in Table 2 and were consistent with literature values reported for chrysophanic acid-9-anthrone and related C. tora anthraquinones [10–12], supporting the identity and purity of the isolate.

Parameter	Observation
Colour / nature	Yellowish-brown crystalline solid
Partition coefficient (oil : water)	9.1
Loss on drying	2.20% w/w
Moisture content	0.50% w/w
Melting point	195 °C
UV λmax	320 nm
TLC Rf value	0.72

Table 2. Physicochemical characterization of the isolated chrysophanic acid-9-anthrone-rich extract.

3.2 Drug–excipient compatibility (FTIR)

FTIR analysis of the extract showed characteristic absorptions consistent with an anthraquinone skeleton, including a carbonyl (C=O) stretch at 1675.3 cm^{-1}, a hydroxyl (O–H) stretch at 3649.0 cm^{-1}, aliphatic C–H stretches at 2924.8 and 2854.0 cm^{-1}, an aromatic C=C stretch at 1571.8 cm^{-1}, and an aromatic C–H bending vibration at 755.5 cm^{-1}. These principal bands were retained, without new peak formation or shift, when the extract was scanned in physical admixture with the selected oil, surfactant and co-surfactant, indicating the absence of any major chemical interaction between the drug and the formulation excipients.

3.3 Optimization of the nanoemulsion

Viscosity and mean droplet size (Z-average) of the five nanoemulsion batches are shown in Figures 1 and 2. Viscosity increased progressively from NE-A1 (4240 cps) through NE-A2 (4430 cps) and NE-A3 (4680

cps) to NE-A4 (4860 cps), broadly tracking the increase in oil-phase concentration and the corresponding decrease in sonication amplitude across these batches. Mean droplet size followed a similar trend, rising from 850.4 nm (NE-A1) to 980.4 nm (NE-A4). On thermodynamic stability testing (centrifugation, heating–cooling and freeze–thaw cycling), NE-A1 and NE-A3 remained homogeneous with no phase separation or creaming, whereas NE-A2 and NE-A4 showed visible instability on at least one stress test (Table 3). Between the two stable batches, NE-A1 combined the lower viscosity with the smaller droplet size and was therefore selected as the optimized nanoemulsion for gel incorporation. The instability of NE-A4 is readily explained by its combination of the highest oil load (10%) and the lowest sonication amplitude (50%) among the five batches — a combination expected to yield coarser, less kinetically stable droplets, consistent with the established relationship between sonication energy input and nanoemulsion droplet size reported for similar oil-in-water systems [24,26]. NE-A2, by contrast, shared an identical oil load (5%) and sonication amplitude (100%) with the stable NE-A1 batch and was processed for a longer sonication time (8 vs 5 min), so its instability cannot be attributed to oil load or processing energy. The principal formulation difference between NE-A2 and NE-A1 was a lower Smix concentration (10% vs 15%; Table 1), which most plausibly explains the instability of NE-A2: a reduced surfactant–co-surfactant fraction would be expected to provide insufficient interfacial coverage to fully stabilize the oil droplets, promoting coalescence despite the additional sonication time.

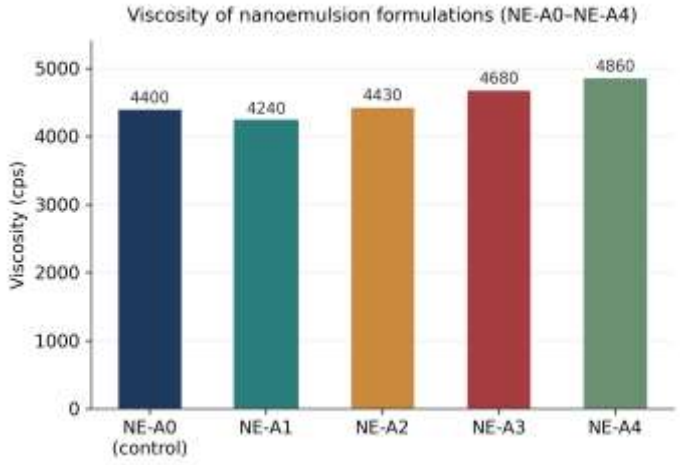

Figure 1. Viscosity of nanoemulsion formulations NE-A0–NE-A4.

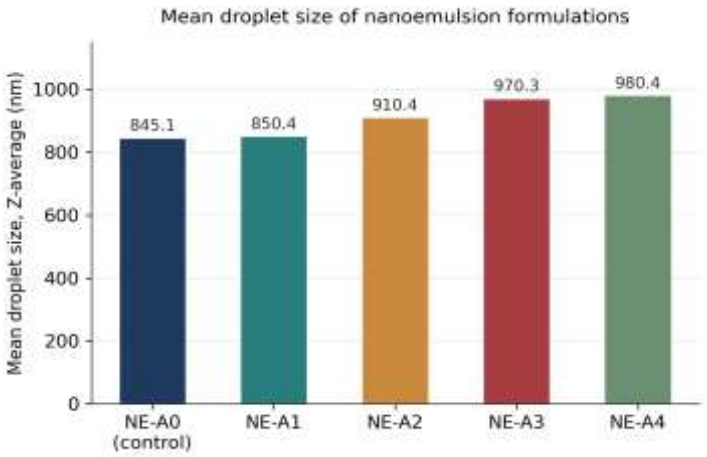

Figure 2. Mean droplet size (Z-average) of nanoemulsion formulations NE-A0–NE-A4.

Batch	Viscosity (cps)	Droplet size (nm)	Centrifugation	Heating–cooling	Freeze–thaw	Outcome
NE-A0	4400	845.1	Pass	Pass	Pass	Stable
NE-A1	4240	850.4	Pass	Pass	Pass	Stable (optimized)
NE-A2	4430	910.4	Fail	Fail	Fail	Unstable
NE-A3	4680	970.3	Pass	Pass	Pass	Stable
NE-A4	4860	980.4	Fail	Pass	Fail	Unstable

Table 3. Viscosity, droplet size and thermodynamic stability outcomes for nanoemulsion batches NE-A0–NE-A4.

3.4 Screening of Carbopol 934 concentration

Blank Carbopol 934 gel bases (GF-1 to GF-4, 1–4% w/w polymer) showed viscosity values between 42,000 and 44,000 cps, with no clear monotonic trend across the tested range (Figure 3), indicating that polymer concentration in this window primarily influenced gel consistency and spreadability rather than producing large viscosity differentials. This range was carried forward for preparation of the nanoemulsion-loaded gels.

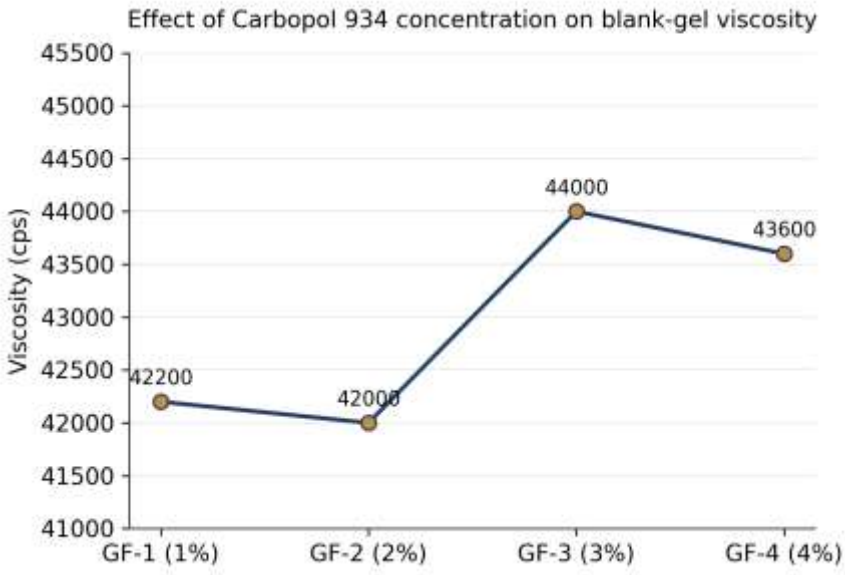

Figure 3. Effect of Carbopol 934 concentration on blank-gel viscosity (GF-1–GF-4).

3.5 Characterization of the nanoemulsion gel

All four nanoemulsion gel formulations (NEG-1–NEG-4) were homogeneous, glossy and free of grittiness, with pH values (6.39–6.50) close to normal skin pH and therefore not expected to cause irritation on topical application (Figure 4a). Viscosity ranged from 42,700 cps (NEG-1) to a maximum of 58,400 cps (NEG-3), with NEG-2 intermediate at 44,000 cps (Figure 4b). NEG-2 showed the greatest spreadability (4.0 cm) and among the better swelling indices (16%) and extrudability values, alongside

the highest drug content (93.55%) of the four batches (Figure 4c–f, Table 4). Taken together, this combination of favourable spreadability, adequate but not excessive viscosity, and the highest drug content identified NEG-2 as the optimized nanoemulsion gel formulation, and it was carried forward for release, antifungal and stability evaluation.

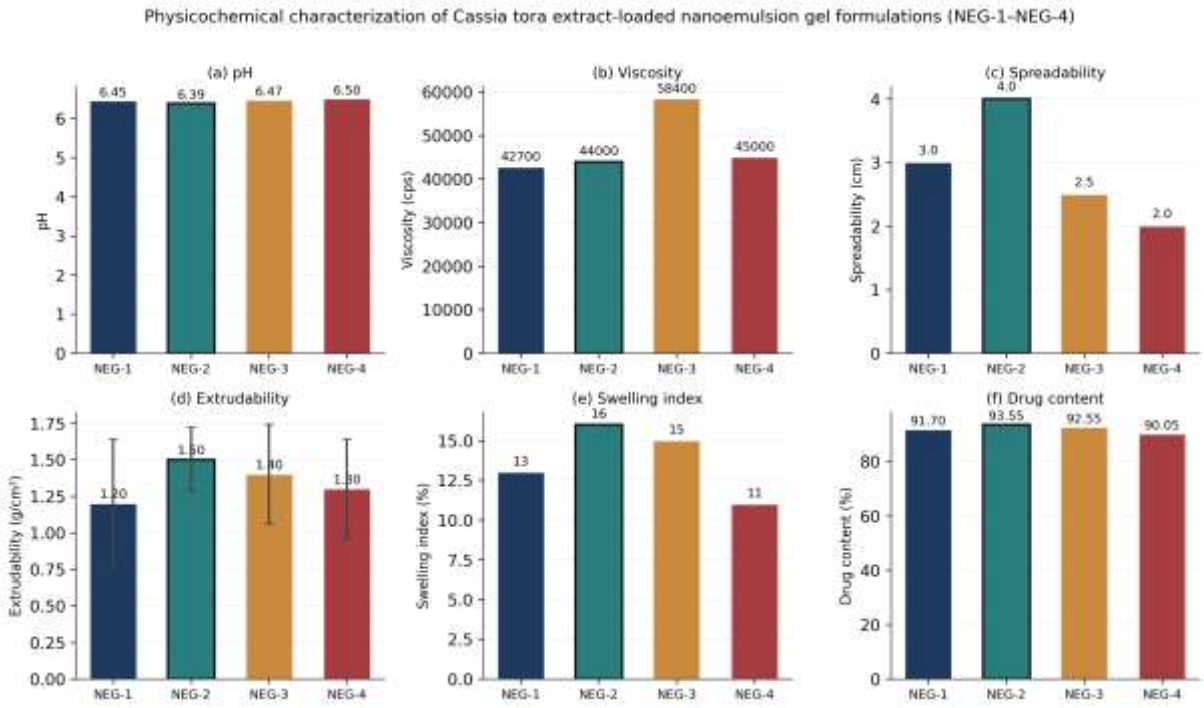

Figure 4. Physicochemical characterization of nanoemulsion gel formulations NEG-1–NEG-4: (a) pH; (b) viscosity; (c) spreadability; (d) extrudability; (e) swelling index; (f) drug content.

Batch	pH	Viscosity (cps)	Spreadability (cm)	Extrudability (g/cm²)	Swelling index (%)	Drug content (%)
NEG-1	6.45	42,700	3.0	1.20 ± 0.44	13	91.70
NEG-2	6.39	44,000	4.0	1.50 ± 0.22	16	93.55
NEG-3	6.47	58,400	2.5	1.40 ± 0.34	15	92.55
NEG-4	6.50	45,000	2.0	1.30 ± 0.34	11	90.05

Table 4. Physicochemical characterization of nanoemulsion gel formulations NEG-1–NEG-4 (mean, n = 3).

3.6 In vitro drug release

Cumulative drug release profiles for NEG-1–NEG-4 are shown in Figure 5. NEG-2 released drug more rapidly across the entire study period, reaching 25.6% at 30 min and 42.6% at 120 min, compared with 36.8–39.6% for NEG-1, NEG-3 and NEG-4 at the same end point. This faster, higher release from NEG-2 is consistent with its comparatively lower cross-link density/optimum polymer concentration allowing easier diffusion of nanoemulsion droplets through the gel network to the membrane, reinforcing its

selection as the optimized batch. The overall release pattern — a comparatively rapid early phase giving way to a slower, near-linear release out to 120 minutes — is consistent with diffusion-controlled release typical of nanoemulsion-based gel systems reported for other actives [20,23].

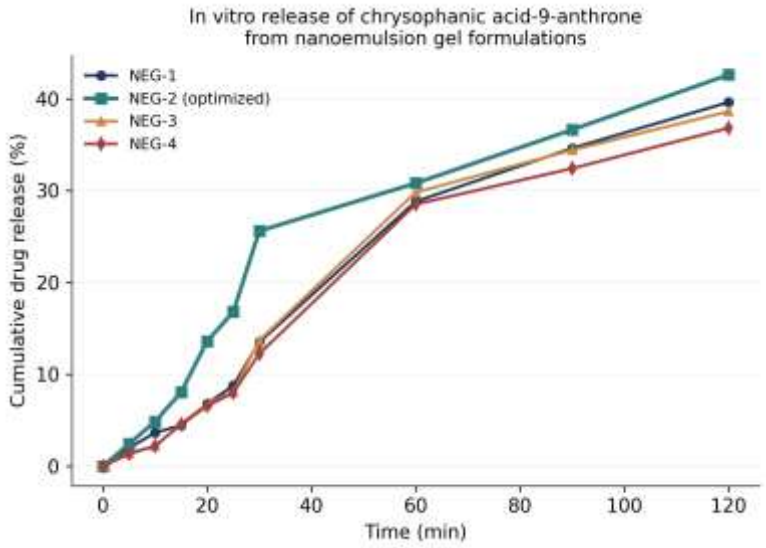

Figure 5. In vitro cumulative release of chrysophanic acid-9-anthrone from nanoemulsion gel formulations NEG-1–NEG-4 across an egg-membrane diffusion barrier (37 ± 0.5 °C).

3.7 In vitro antifungal activity

The optimized gel (NEG-2) showed clear, concentration-dependent antifungal activity against Aspergillus niger MTCC 282 (Figure 6), with the zone of inhibition increasing from 8.7 ± 0.6 mm at 25 µg/mL to 12.3 ± 1.2 mm at 50 µg/mL, 15.2 ± 1.6 mm at 75 µg/mL, and 22.0 ± 1.7 mm at 100 µg/mL, approaching the 26.0 mm zone produced by the amphotericin B reference standard (10 µg/mL). This concentration–response relationship confirms that the antifungal activity previously reported for crude C. tora extracts [6–9] is retained, and indeed appears efficiently delivered, when the isolated chrysophanic acid-9-anthrone fraction is formulated as a nanoemulsion gel, supporting the therapeutic rationale for this delivery approach.

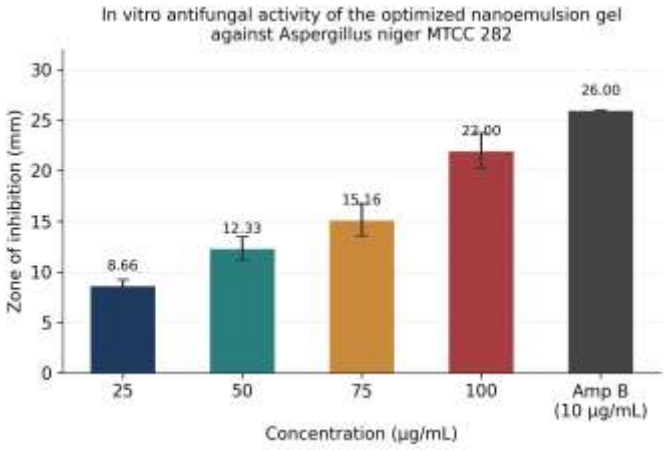

Figure 6. In vitro antifungal activity (zone of inhibition) of the optimized nanoemulsion gel (NEG-2) against Aspergillus niger MTCC 282, relative to amphotericin B.

3.8 Stability studies

Over 3 months of storage, NEG-2 remained entirely stable at 37 ± 2 °C/65% RH — the recommended long-term storage condition — with no measurable change in pH or drug content (93.55% at months 1, 2 and 3; Figure 7). At the accelerated stress conditions of 45 °C/75% RH and 60 °C, a modest, temperature-dependent decline in drug content (to 91.0% and 90.1% of label claim, respectively, at 3 months) and a small downward drift in pH were observed, but no phase separation, creaming or visible degradation occurred at any condition, indicating that the formulation possesses adequate short-term physical and chemical stability for further pharmaceutical development.

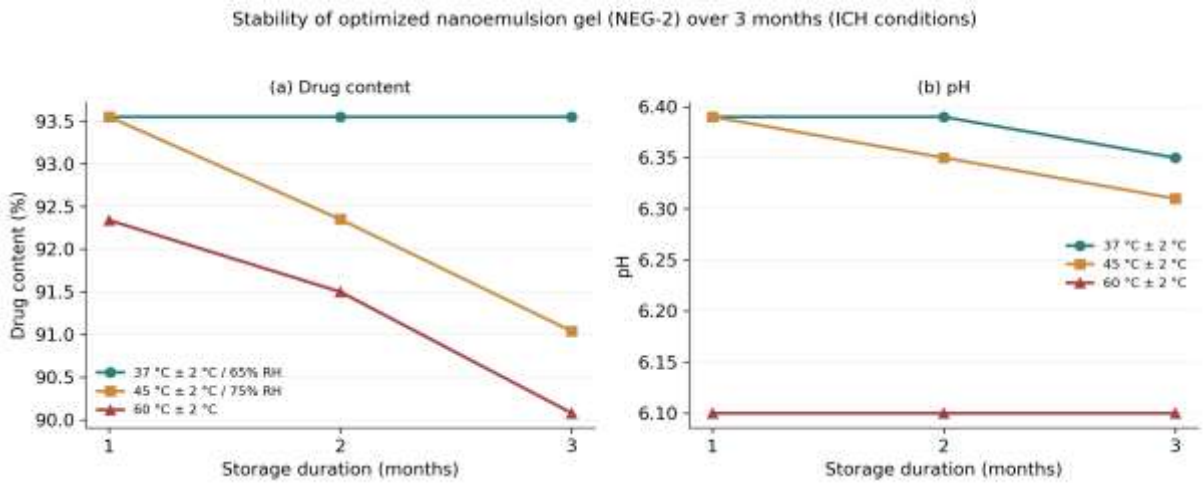

Figure 7. Stability of the optimized nanoemulsion gel (NEG-2) over 3 months under ICH-type storage conditions: (a) drug content; (b) pH.

3.9 Overall discussion

Collectively, these results indicate that ultrasonication-assisted nanoemulsification can convert a poorly water-soluble, plant-derived antifungal anthraquinone into a small-droplet, thermodynamically stable oil-in-water carrier, and that this nanoemulsion can in turn be formulated into a Carbopol 934 gel with skin-compatible pH, favourable rheology, and drug-release and antifungal performance that compare well with previously reported nanoemulsion-gel systems for synthetic antifungal and anti-inflammatory drugs [20–23]. The principal limitation of the present work is that all efficacy and release data are derived from in vitro and ex vivo membrane models; confirmation in a validated skin-permeation model (e.g., excised animal or reconstructed human skin) and in an in vivo dermatophyte infection model, together with a full ICH long-term stability protocol and a broader antifungal panel extending beyond A. niger to clinically relevant dermatophytes such as Trichophyton and Microsporum species, will be necessary before clinical translation can be considered.

4. Conclusion

A nanoemulsion gel loaded with chrysophanic acid-9-anthrone isolated from Cassia tora seed was successfully developed and optimized. The optimized nanoemulsion (NE-A1) and gel (NEG-2) combined an acceptably small droplet size, skin-compatible pH, favourable spreadability and rheology, sustained in vitro drug release, concentration-dependent antifungal activity against Aspergillus niger, and short-term physicochemical stability. These findings support the technical feasibility of this plant-derived nanocarrier

as a topical antifungal alternative and provide a basis for further ex vivo permeation, in vivo efficacy, and extended stability studies ahead of clinical development.

References

1. Rippon JW. Medical Mycology: The Pathogenic Fungi and the Pathogenic Actinomycetes. 3rd ed. Philadelphia: Saunders; 1988. p. 140–275.
2. Breden KP. Superficial fungal infection. Pediatr Rev. 2012;33(22).
3. Chakraborty T, Saini V. Antifungal gel: for different route of administration and different drug delivery system. Int J Biopharm. 2014;5(3):230–40.
4. Moghimipour E, Ameri A. Formulation of an antidermatophyte cream from hydroalcoholic extract of Eucalyptus camaldulensis leaves. Jundishapur J Nat Pharm Prod. 2009;4(1):30–40.
5. Renesheya Joy Jeba Malar T, Johnson M. Antifungal and antibacterial activity of Aloe vera extract. Int J Biomed Adv Res. 2012;3(3):184–7.
6. Jain S, Dubey P. Antifungal properties of weed plant C. tora on dermatophytosis. Int J Chem Sci. 2012;1:1451–8.
7. Dubey P, Seth R. Antifungal properties of seeds of Cassia tora Linn. Hortic Int J. 2018;2(6):299–301.
8. Pawar HA, D'Mello P. Antifungal activity of methanolic extract of Cassia tora leaves against Candida albicans. Int J Res Ayurveda Pharm. 2018;2(3):793–6.
9. Supare S, Patil M. Estimation of phytochemical components from Cassia tora and to study its larvicidal activity. Int J Pharm Sci Invent. 2015;4(6):11–6.
10. Acharya TK, Chatterjee IB. Isolation of chrysophanic acid-9-anthrone, a fungicidal compound from Cassia tora. Sci Cult. 1974;40:376.
11. Raghunathan K, Hariharan V, Rangaswami S. Chrysophanol-1-β-gentiobioside, a new anthraquinone glycoside from Cassia tora Linn. Indian J Chem. 1974;12:1251–3.
12. Miyuki K, Morishita E, Shibata S. Constituents of Cassia tora L.: glucosides of rubrofusarin. Chem Pharm Bull. 1969;17:458.
13. Kirtikar KR, Basu BD. Indian Medicinal Plants. Vol II. Delhi: Periodical Experts D-42, Vivek Vihar; 1975. p. 877.
14. Hooker JD. The Flora of British India. Vol II. England: L. Reeve and Co.; 1879. p. 26.
15. Savardekar P, Bajaj A. Nanoemulsions: a review. Int J Res Pharm Chem. 2016;6(2):312–22.
16. Yadav U, Prajapati SK. Development, optimization, and characterization of topical nanoemulsion gel of an antifungal agent for effective treatment of onychomycosis. Asian J Med Pharm Sci. 2013;1(1):12–21.
17. Chellapa P, Mohammed AT. Nanoemulsion and nanogel as a topical formulation. IOSR J Pharm. 2015;5(10):43–7.
18. Hussain A, Samad A, Singh SK, et al. Nanoemulsion gel-based topical delivery of an antifungal drug: in vitro activity and in vivo evaluation. Drug Deliv. 2014;1:1–16.
19. Valenta C, Schultz K. Influence of carrageenan on the rheology and skin permeation of microemulsion formulations. J Control Release. 2004;95:257–65.
20. Singh R, Chakravorty A, Kumar P, Chaturvedi A. Nanoemulsion: an effective therapy for transdermal drug delivery. Res J Biol. 2013;3:33–8.
21. Modi JD, Patel JK. Nanoemulsion-based gel formulation of aceclofenac for topical delivery. Int J Pharm Pharm Sci Res. 2011;1(1):6–12.

22. Singh VK, Singh PK. Formulation and evaluation of topical gel of aceclofenac containing piperine. Indo Am J Pharm Res. 2013;3(7):5266–80.
23. Shakeel F, Baboota S, Ahuja A, Ali J, Shafiq S. Skin permeation mechanism and bioavailability enhancement of celecoxib from transdermally applied nanoemulsion. J Nanobiotechnology. 2008;6:8.
24. Lawrence MJ, Rees GD. Microemulsion-based media as novel drug delivery systems. Adv Drug Deliv Rev. 2000;45:89–121.
25. McClements DJ. Nanoemulsions versus microemulsions: terminology, differences, and similarities. Soft Matter. 2012;8:1719–29.
26. Leong TSH, Wooster TJ, Kentish SE, Ashokkumar M. Minimising oil droplet size using ultrasonic emulsification. Ultrason Sonochem. 2009;16:721–7.